

# Design and application of over-flexion–extension position mould based on computed tomography examination of nasal bone patients

L. Yang<sup>1</sup>, C. Yang<sup>2\*</sup>, G. Gao<sup>1</sup>, Y. Li<sup>1</sup>, L. Gao<sup>1</sup>, Q. Qi<sup>3</sup>, X. Li<sup>1</sup>, Ch. Yang<sup>3</sup>

<sup>1</sup>Department of Medical imaging, The second hospital of Hebei Medical University, Shijiazhuang 050000, China

<sup>2</sup>Department of medical equipment, The second hospital of Hebei Medical University, Shijiazhuang 050000, China

<sup>3</sup>College of Forensic Medicine, Hebei Medical University, Shijiazhuang 050000, China

## ► Technical note

### \*Corresponding author:

Cun Yang, ME,

### E-mail:

[yangcun2020k@126.com](mailto:yangcun2020k@126.com)

Received: May 2023

Final revised: October 2023

Accepted: November 2023

*Int. J. Radiat. Res., October 2024;*  
22(4): 1075-1078

DOI: 10.61186/ijrr.22.4.1075

**Keywords:** Nasal bone, over-flexion-extension, mould, computed tomography, cervical spine.

## INTRODUCTION

The nasal bone is located in the most prominent part of the face, so when facial trauma occurs, the nasal bone is particularly vulnerable to fracture<sup>(1)</sup>. The complex geometry and many structures of the nose and the existence of bone sutures and variations between adjacent structures make it difficult to diagnose and classify nasal bone fractures, leading to misdiagnosis and missed diagnosis. X-ray is the most commonly used method in the diagnosis of nasal bone fractures, but its accuracy is affected by the overlapping of facial bone structures on plain film. In recent years, the wide application of computed tomography (CT) three-dimensional imaging technology, has provided a reliable tool for the diagnosis of nasal bone fractures<sup>(2)</sup>. At present, in the process of medical imaging CT examination, scans are often taken in special positions. Some patients need to lower and raise their heads to the maximum extent during the examination process, forming medical hyperflexion and hyperextension of the cervical spine; however, maintaining this position for an extended period is difficult for patients and can easily cause discomfort. Patients often have difficulty achieving standard flexion or hyperextension without the support of a comfortable mould during the

## ABSTRACT

**Background:** We aimed to develop a mould for the over-flexion and over-extension positions to solve the technical problem of patients who find it difficult to form the over-flexion and over-extension positions of the cervical spine by lowering their heads forwards and raising their heads backwards. **Materials and Methods:** We calculated the average physiological bending radian of normal people and measured the depth of the cervical physiological curve using Borden's method. Finally, we designed a mould that conformed to the characteristics of the human cervical spine to conduct nasal bone examinations in the over-flexion and over-extension positions in combination with the patient's examination position. **Results:** When the neck is equipped with an over-flexion and over-extension mould when performing coronal nasal bone examinations, the nasal bone structure is more fully displayed than in routine examinations; furthermore, the clinical diagnosis efficiency greatly improves, and the rate of misdiagnosis significantly reduces. **Conclusion:** This model increases the comfort of patients and solves the technical problem of patients who cannot maintain the over-flexion and over-extension positions for an extended period.

examination, leading to anomalies in the imaging findings<sup>(3-5)</sup>. Therefore, to improve examination efficiency, it is particularly important to be able to maintain the correct posture<sup>(6-10)</sup>.

In this study, we first created a flexion-extension mould to enable patients to perform flexion and extension of the cervical spine to prevent problems during imaging examination.

## MATERIALS AND METHODS

### General information

In this study, 20 cases of nasal bone fracture were scanned with multi-slice CT (MSCT) using a self-designed hyperflexion and extension mould. The MSCT was performed using an Optima 128 T CT machine (CT660, USA). In the process of designing the hyperextension mould, the CT data of 30 normal people were collected, and the depth from the position of C4 in the sagittal plane to the bed plate was calculated. Image post-processing and hyperextension and flexion scanning of patients with nasal bone fractures were performed using an Advantage Workstation 4.6 (ADW4.6, GE Healthcare, DE). This study was conducted in accordance with the Declaration of Helsinki and approved by the ethics

committee of The second hospital of Hebei Medical University, Approval number is NO. 2020-R251 (3/3/2020). Written informed consent was obtained from all participants.

### Model design

#### Measuring the physiological curvature of the cervical spine

In this study, the physiological curvature of the cervical spine was measured using Borden's method. A plane model of the normal cervical curvature was established and the depth of the cervical physiological curve was the basis for the size of the mould.

In Borden's measurement method, it is generally believed that the position of the apex of the curvature arc of the cervical spine should be at C4, as shown in figure 1. Taking point O as the coordinate origin to determine the coordinates of A, B and C ( $[X_n, Y_n], n \leq 3$ ) to draw a full circle, a line is drawn from the posterior upper edge of the odontoid process of the axis to the posterior lower edge of the C7 vertebral body using CAXA (2011) design software. The straight line is the AB line, and a connecting line is drawn along the posterior edge of each vertebral body of the cervical spine (the AB arc). The vertical cross line at the widest point between the AB line and the AB arc is the C line, which is the depth of the physiological curve of the cervical spine.  $\angle AOB$  is the physiological curvature of the cervical spine (11). A circular model is calculated based on three coordinate points; the coordinates of the centre of any circle are set as  $(x_0, y_0)$  and the radius is  $r$ . Then, as shown in figure 1, the equation of the circle can be written as:

$$(x_1 - x_0)^2 + (y_1 - y_0)^2 = r^2, \quad (1)$$

$$(x_2 - x_0)^2 + (y_2 - y_0)^2 = r^2 \text{ and} \quad (2)$$

$$(x_3 - x_0)^2 + (y_3 - y_0)^2 = r^2, \quad (3)$$

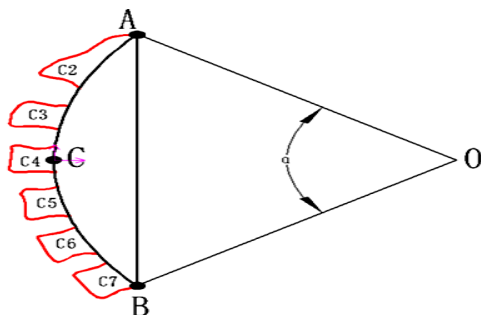


Figure 1. Schematic diagram of cervical curvature.

### Materials

The internal support material was made of palm material, and the outer layer was wrapped with silicone cushioning fabric to increase the comfort of the user.

### Structural design

The over-flexion and over-extension mould is

assembled by fastening and pasting the support, support structure and base. The semi-circular arc on the lower side aligns perfectly with the CT examination bed, and a fixed connection device is added so that the mould can be connected rigidly to the body of the bed, including the pedestal and supporting structure, during the installation process. A cervical spine fixation groove is designed above the mould, and the lower part of the mould is connected to the examination bed. A head baffle is arranged on the upper part of the mould in the post-buckling position to act as a head fixing plate.

### Application method

Twenty patients were fitted with a flexion-extension mould at the neck during coronal nasal bone examination. The parameters for MSCT scanning were as follows: tube current = 180 mA, slice thickness = 0.625 mm, slice distance = 0.312 mm, pitch = 0.516:1, rack speed = 1 s, scanning field = 12 cm, reconstruction interval = 0.625 mm. The patients were scanned in the supine position, and the auditory canthus line was scanned vertically on the bed's surface. The scanning range was from the upper orbital margin to the level of the hard palate (including the entire maxilla). Patients adopted the supine position, with their heads tilted backwards, and the mould was applied to the neck so that the canthus line was parallel with the scanning bed. The scanning range was the base of the nose to the maxillary frontal process.

At the end of scanning, the patients were questioned about the degree of comfort of the mould. After two doctors from the medical imaging department evaluated the images, the evaluation criterion was whether the nasal interosseous gap, nasomandibular suture, fracture line and fracture condition were clearly displayed. The potential maximum score was 5.

### Statistical analysis

A data analysis was performed using SPSS 22.0 statistical software. Measurement data conforming to a normal distribution were expressed in the form of mean  $\pm$  standard deviation ( $x \pm s$ ) and compared using an independent-samples  $t$  test.

## RESULTS

### Patients' satisfaction and the result of the scanned images

In a survey of patients' satisfaction with the use of our hyperextension and flexion moulds, all 20 patients were satisfied with the comfort of the moulds, with a satisfaction rate of 100%. The average value of the C line was  $60 \pm 5$  mm and the height of the mould at the cervical vertebra was designed to be 100 mm. The depth of the cervical spine needed to

accommodate the different patients in the hyperextension mould is shown in figure 2. The scanned image after using the mould is shown in figure 3.

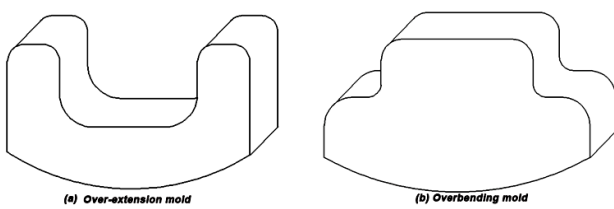


**Figure 2.** The view to over-extension mold and overbending mold. **a)** Over-extension mold. **b)** Overbending mold.

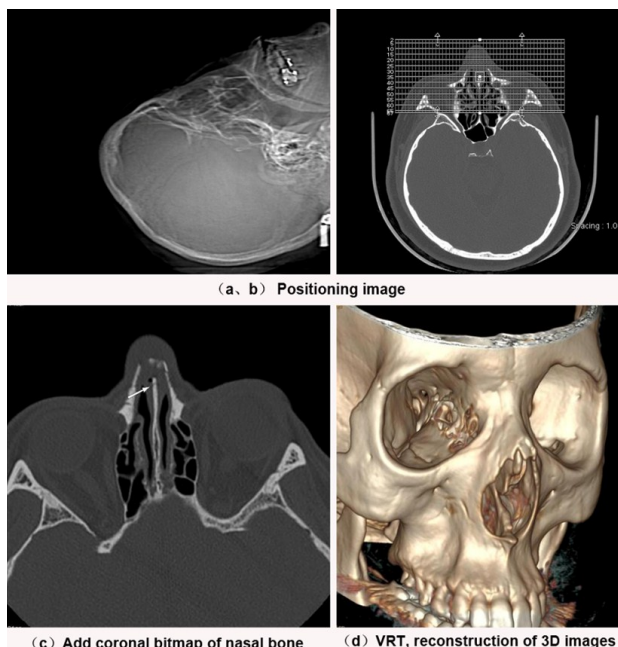


**Figure 3.** CT nasal bone plain scan and three-dimensional reconstruction. **a, b)** Supine position head back coronal scan lateral positioning images and scan lines. **c)** The coronal scan image of the nasal bone in the supine position with the head tilted back shows that the continuity of the bone in the front part of the nasal septum is interrupted, and there is no obvious misalignment and angulation. **d)** VRT image, reconstructed three-dimensional image, showing bilateral distal nasal bone collapse.

The figure 3 showed that the distal end of the nasal bone had collapsed on both sides, several fracture lines were seen, the broken end was slightly displaced, and small bone fragments were seen on the left side. The anterior part of the nasal septum was interrupted, and no obvious dislocation or angulation was found. The soft tissues around the nose were swollen, air had accumulated, and the soft tissues of the nasal dorsum and nasal vestibule were clearly swollen and thickened.

#### Improving diagnostic accuracy

Compared with previous models, our invention fixes the support firmly to the examination bed before the examination through the joint use of the support, the three support rods and the fastening

mechanism. The support rod is adjusted when the over-flexion position is checked, the middle support bar is slid down, and the support bars on both sides are slid up to form a lower concave structure, which is fixed by a fastening mechanism. When checking the buckling position, the support bar is adjusted so that the middle support bar slides up and both sides of the support bar slide down to form a convex structure, which is fixed by the fastening mechanism. During the examination, the patient can achieve the flexion-extension position by fitting the strut to the cervical spine as much as possible. The patient's neck is not suspended because of the support from both the strut and the support rod. The support rod can be attached to help the patient remain upright and maintain the flexion or hyperextension position for an extended period to reduce both discomfort and the difficulty of reaching over-flexion or over-extension. Even with a long examination, the muscles in the patient's neck will not become tired or start trembling; thus, it is advantageous for enabling cooperation with the examination, reducing the examination time, obtaining clearer and more accurate imaging results and improving the interpretation accuracy of the results.

#### Image quality rating by radiologists

The image quality of the 20 data groups was evaluated by two doctors in the medical imaging department, and an independent-samples t test was performed on the scoring data. When the effective score of the experts was 20, the results showed that there was no significant difference between the mean scores of the two experts ( $4.85 \pm 0.36635$  vs  $4.80 \pm 0.41039$ ,  $P = 0.687$ ), which demonstrated that the two experts had the same opinion in terms of image display quality. The scores and test results are shown in table 1.

**Table 1.** Statistical score table of 2 radiologists.

|       | Group   | N  | Average | Standard deviation | T value | P value |
|-------|---------|----|---------|--------------------|---------|---------|
| Score | Expert1 | 20 | 4.8500  | 0.36635            | 0.406   | 0.687   |
|       | Expert2 | 20 | 4.8000  | 0.41039            |         |         |

## DISCUSSION

In this paper, a type of mould for aiding flexion and extension in medical imaging examination was developed. In the current existing examination methods, patients need to lower and raise their heads excessively, which makes it difficult for them to form flexion and extension in the cervical spine. This research has solved this technical problem.

When undergoing physical examinations with CT machines and other equipment, sometimes, the patient will be required to lower their head forwards and raise it backwards, forming cervical flexion and extension. However, these postures are difficult for some patients. On the one hand, sometimes due to

discomfort, patients cannot reach the over-flexion or over-extension position, while on the other hand, even when the examination time is slightly extended, it is difficult to stand up. Even if the examination process is prolonged, this increases patients' discomfort and also causes patients' necks to tremble or shake. The final image is blurred because of motion shadows, which affects the inspection effect.

In Yahyazadehfar's research (12), a generalised equation was developed for an inset CT specimen that describes the stress intensity within the inset material for mode I loading. The inset CT approach has been adopted and used successfully in previously reported evaluations of the fracture behaviour of human enamel (13-16). In our study, we measured the depth of the cervical physiological curve using Borden's measurement method, and we innovatively developed an external supporting mould. At the same time, the current research mainly focuses on the over-flexion-extension X-ray evaluation of the human thoracolumbar spine under compressive preload and the physiological curvature of the spine (17,18). Because of the spatial limitations of CT, research on over-flexion-extension in CT is lacking. Therefore, we developed an over-flexion-extension position mould that is vital to the CT examination of nasal bone patients.

In conclusion, the use of our mould in the coronal joint transverse scan can fully show the different directions of the fracture line, and the two play a complementary role. It can fully display the anatomic structure of the nose, observe the affected area comprehensively and improve diagnostic accuracy, and it is also of great help in forensic identification. The mould allows the patient to undergo examination while maintaining a specific body position for an extended period during the examination and is beneficial to the doctor by ensuring the cooperation of the patient. Shortening the examination time can also facilitate clearer and more accurate clinical images and improve the accuracy of the results (11,19,20).

## CONCLUSION

The design of the over-flexion and over-extension mould improves the comfort of patients. It is of great significance for the application of nasal bone patients and the examination of over-flexion and over-extension.

## ACKNOWLEDGMENT

*Not applicable.*

**Competing interests:** All of the authors had no any personal, financial, commercial, or academic conflicts of interest separately.

**Funding:** The project was supported: Youth Science and Technology Project of Hebei Provincial Health and Family 3. Planning Commission, NO.20210815.

**Ethics approval and consent to participate:** This study was conducted in accordance with the Declaration of Helsinki and approved by the ethics committee of The second hospital of Hebei Medical University, Approval number is NO. 2020-R251 (3/3/2020). Written informed consent was obtained from all participants.

**Authors' contributions:** Y.L. and Y.C. conceived of the study and G.G., L.Y. and G.L.J. participated in its design and data analysis and statistics and Q.Q., L.X and Y.C.T. helped to draft the manuscript. All authors read and approved the final manuscript.

## REFERENCES

1. Hwang K, You SH, Kim SG, Lee SI (2006) Analysis of nasal bone fractures; a six-year study of 503 patients. *J Craniomaxillofac Surg*, **17(2)**: 261-264.
2. Hwang K, Jung JS, Kim H (2018) Diagnostic performance of plain film, ultrasonography and computed tomography in nasal bone fractures: A systematic review. *Plast Surg (Oakv)*, **26(4)**: 286-292.
3. Chen SQ, Huang ZP, Wang JF, Deng XY, Liu DF (2016) To improve the image quality of nasal bone CT scan. *Modern Medical Imaging*, **25 (06)**: 1100-1102.
4. Jang Y (2020) Comparison of the clinical value of X-ray plain film and CT in the diagnosis of nasal bone fracture. *Chinese community physicians*, **36(21)**: 140-141.
5. Wang MW, Tan SL, Liu X, Wan L (2017) The study of MSCT image post-processing display and diagnosis of nasal region fracture. *China judicial identification*, **6**: 56-60.
6. Wang N, Li M, Wang J, Zhang ZX, Qu Y (2018) Clinical study of Gukang capsule in promoting the recovery of nasal bone fracture. *Chinese Clinical Pharmacology Magazine*, **34(21)**: 2500-2502.
7. Shen SH, Mar L, Fu Z, Geng FQ, Chen C (2018) The clinical value of high frequency ultrasound in the diagnosis of nasal bone fracture and guided closed reduction. *Chinese Journal of Ultrasound Imaging*, **10**: 914-915.
8. Zhao XL (2010) Forensic identification of nasal bone fractures. *Chinese Journal of Forensic Medicine*, **25(4)**: 293,296,298.
9. Tang XX, Zhang J, Zhang AC, Zhang Q (2014) Emergency diagnosis and treatment of nasal bone fracture with different classification. *Chinese Journal of Emergency Medicine*, **23(2)**: 219-221.
10. Zhou ZJ, Gao B, Chao HM (2008) Multi-slice spiral CT and post-processing technique in the diagnosis of nasal bone fracture. *Chinese Journal of Medical Computer Imaging*, **14(04)**: 299-302.
11. Zhu WB (2010) The effect of spinal fine-tuning manipulation in the treatment of cervical curvature straightening and reverse arch. *Chinese Journal of Orthopaedics and Traumatology of Traditional Chinese Medicine*, **18(11)**: 34-35.
12. Bajaj D and Arola D (2009a) Role of prism decussation on fatigue crack growth and fracture of human enamel. *Acta Biomater*, **5(8)**: 3045-3056.
13. Bajaj D and Arola DD (2009) On the R-curve behavior of human tooth enamel. *Biomat*, **30(23-24)**: 4037-4046.
14. Bajaj D, Nazari A, Eidelman N, Arola DD (2008) A comparison of fatigue crack growth in human enamel and hydroxyapatite. *Biomaterials*, **29(36)**: 4847-4854.
15. Tawackoli W, Marco R, Liebschner MA (2004) The effect of compressive axial preload on the flexibility of the thoracolumbar spine. *Spine (Phila Pa 1976)*, **29(9)**: 988-993.
16. Vlok AJ, Naidoo S, Kamat AS, Lamprecht D (2018) Evaluation of locally manufactured patient-specific custom-made implants for cranial defects using a silicone mould. *S Afr J Surg*, **56(3)**: 38-42.
17. Yahyazadehfar M, Bajaj D, Arola DD (2013) Hidden contributions of the enamel rods on the fracture resistance of human teeth. *Acta Biomater*, **9(1)**: 4806-4814.
18. Yahyazadehfar M, Nazari A, Kruczik JJ, Quinn GD, Arola D (2014) An inset CT specimen for evaluating fracture in small samples of material. *J Mech Behav Biomed Mater*, **30**: 358-368.
19. Tao H, Chen C, Zhang HY, Qu XX, Guo J, Xian JF (2021) Establishment and clinical efficacy evaluation of depth learning model of nasal bone fracture. *Radiology in Practice*, **36(08)**: 959-964.
20. Ma L and Shen SH (2021) A visual study of closed reduction of nasal bone fracture monitored by ultrasound during the whole process. *Journal of Medical Imaging*, **31(05)**: 744-749.